Radiotracer Measurement of Local Deposition Profiles, Friction Reentrainment, and Impaction Reentrainment in an Electrostatic Precipitator

A radiotracer-based method of measuring local particle deposition profiles and reentrainment rates in an electrostatic precipitator has been developed and demonstrated. In tests performed on a pilot-scale precipitator, differences in local deposition profiles obtained with and without a predeposited layer of dust on the plate were observed. Rates of reentrainment due to gas friction (aerodynamic drag) and to particle impaction on the plate were measured separately, and correlated with a semiempirical formula. Both friction and impaction reentrainment rates were found to vary as powers of the difference between the gas velocity and a minimum velocity required for reentrainment. The impaction reentrainment was found to vary as a power of the inlet dust loading.

RICHARD. M. FELDER and ENRIQUE ARCE-MEDINA

Department of Chemical Engineering
North Carolina State University
Raleigh, NC 27695

SCOPE

Electrostatic precipitators are generally designed by analogy with similar operating units. Unfortunately, precisely analogous conditions (gas flow, temperature and pressure, dust loading, dust resistivity, particle size distribution, etc.) in two different process streams are rarely encountered, so that some degree of extrapolation is always required. Several empirical correlations of collection efficiency with various experimental parameters exist (Oglesby and Nichols, 1978), but they are imprecise, and relatively conservative overdesign procedures must therefore be used to arrive at a final precipitator design.

A number of mathematical models of electrostatic precipitators have been developed in recent years. The intent of these models is to enable the prediction of particle collection efficiencies from specified values of feed parameters (air flow rate, dust loading, and physical properties of the dust) and precipitator operating conditions (plate area and spacing, corona wire spacing, applied voltage, temperature and pressure). An accurate model of this nature would serve as an ideal basis for design or scale-up of a precipitator to operate at conditions different from those for which data already exist.

In their present state of development, however, these models can do little more than provide qualitative estimates of collection efficiencies for given sets of conditions. The inadequacies could be due in part to violations of the model assumptions regarding electrical field distributions, particle charging mechanisms, and ion and charged dust particle migration rates, and in part to the failure of the models to account correctly for such phenomena as sweepage and reentrainment.

An experimental technique to elucidate these matters has been developed. A pulse of a radioactive dust or fly ash is used as a tracer to measure local dust deposition profiles on the collection plate, as well as local rates of reentrainment, both due to gas friction (aerodynamic drag) and particle impaction. The local deposition profile provides a sensitive basis for evaluation of model predictions—much more sensitive than the overall collection efficiency, which is normally the only datum available. The measured friction and impaction reentrainment rates can be correlated with dust properties and precipitator operating conditions, thus providing a basis for accurate representation of these phenomena in precipitator models.

In preliminary tests demonstrating this technique, fly ash samples were irradiated in a nuclear reactor, and were injected at the inlet of a pilot-scale electrostatic precipitator. Local deposition profiles and reentrainment rates were measured for a narrow range of experimental conditions. A description of the experimental method and a summary of results are given by Felder and Arce-Medina (1980). In subsequently performed experiments, rates of both friction and impaction reentrainment were measured and correlated with various precipitator operating parameters, including gas flow rate, inlet dust loading, and the absence or presence of a predeposited layer of dust on the collection plate. The results of these experiments are the subject of the present paper. A more complete description of the experiments and data analysis is given by Arce-Medina (1982).

Correspondence concerning this paper should be addressed to R. M. Felder.
E. Arce-Medina is presently at the Department of Chemical Engineering, National Polytechnic Institute, Mexico City, Mexico.

CONCLUSIONS AND SIGNIFICANCE

The radiotracer method described in this study provides a means of measuring local particle deposition profiles and both friction and impaction reentrainment rates in a wire-plate electrostatic precipitator.

The particle migration velocity in a precipitator is reduced as the layer of dust on the collection plate increases in thickness. This reduction is manifested by a downstream shift in the point of maximum particle deposition for dust particles entering a stage at a fixed distance from a collection plate.

Reentrainment may be modeled as a first-order process, with the rate constant serving as a measure of the reentrainment rate. The rate of reentrainment increases with increasing gas velocity, and for a given velocity, the rate is lower when a dust layer covers the plate than when the plate is clean. The latter result is consistent with an observation of Zimon (1969) that autohesive forces binding collected dust particles to each other tend to be stronger than adhesive forces binding particles to the plate. The rate of impaction reentrainment increases with both gas velocity and inlet dust loading for both clean and coated plates.

The minimum gas velocity at which reentrainment is observed to occur is approximately 1.5 m/s for friction reentrainment from both clean and coated plates. The minimum velocity for impaction reentrainment is also about 1.5 m/s for clean plates, but decreases for coated plates. For the level of predeposition used in this study (which could not be quantified), the minimum velocity dropped to about 1.3 m/s.

A semiempirical relationship proposed by Zimon (1969) provides a reasonable basis for correlating the variations in reentrainment rate with gas velocity and dust loading. For both clean and coated plates, the rate of friction reentrainment varies as approximately the 1.15th power of the difference between the gas velocity and the minimum velocity required for reentrainment. The impaction reentrainment rate varies linearly with the velocity difference, and with a power of the inlet dust loading. The power was found to be close to 3 for clean plates, and close to 2 for coated plates. However, little significance should be attached to these numerical values; a much larger data base will be required to provide statistical significance to the regression estimates.

EXPERIMENTAL SYSTEM AND PROCEDURES

Experiments were performed on the pilot-scale electrostatic precipitator located at the National Environmental Research Center, Research Triangle Park, NC (Lawless et al., 1979). A schematic diagram of the experimental system is shown in Figure 1.

The collection plates of the precipitator are 1.2 m square, and the plate-to-plate spacing can be varied from 12.7 to 38 cm. The specific collector area of the ESP is 28 $m^2/m^3 \cdot s$ at a plate spacing of 23 cm and a gas velocity of 1.5 m/s. There are four electrical sections and one channel for gas flow. The precipitator has the capability of running either at ambient or elevated temperatures. In the studies performed, only ambient operation was used.

A 3.2 cm scintillation crystal and photomultiplier base (RCA 6342A) with a built-in preamplifier (ORTEC 276) was mounted behind the collection plate in the second stage of the unit. The detector mount was suspended from a horizontal rod parallel to the direction of flow in the precipitator, so that the detector could be moved horizontally from one end of the plate

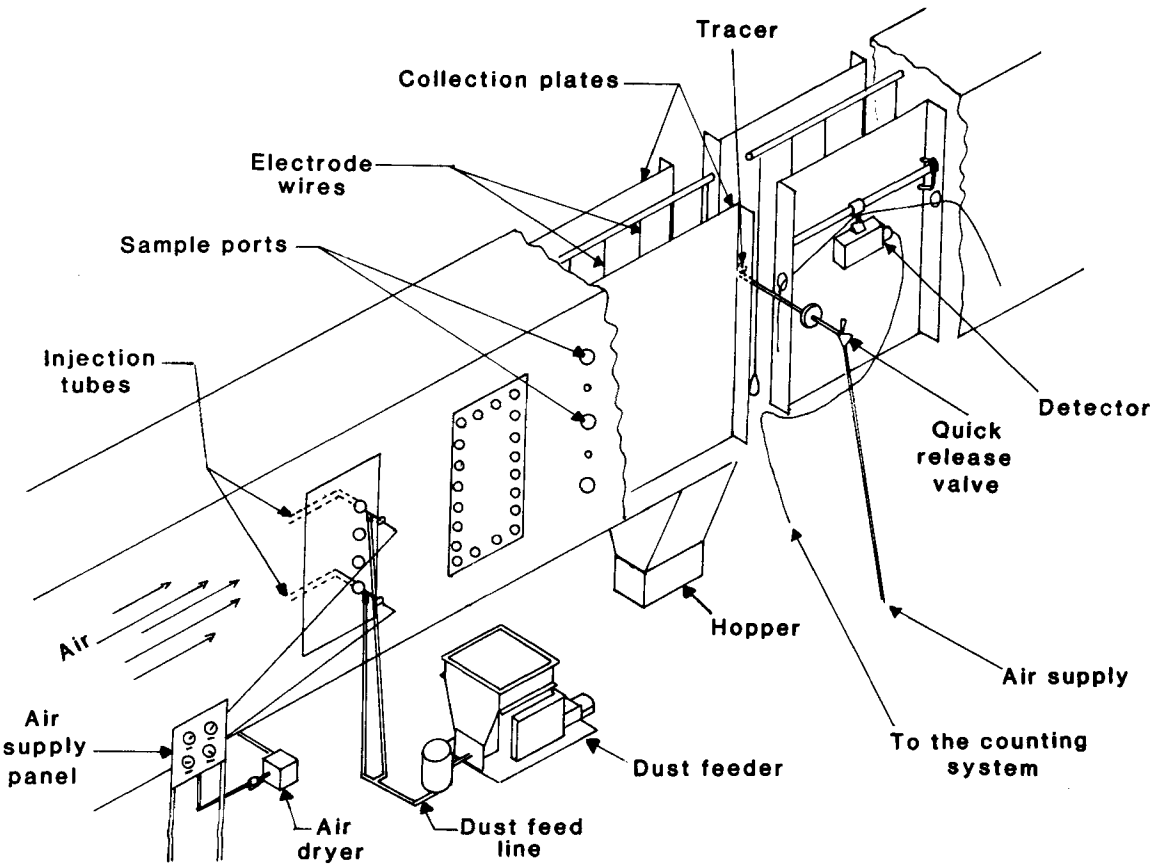

Figure 1. Pilot-scale electrostatic precipitator.

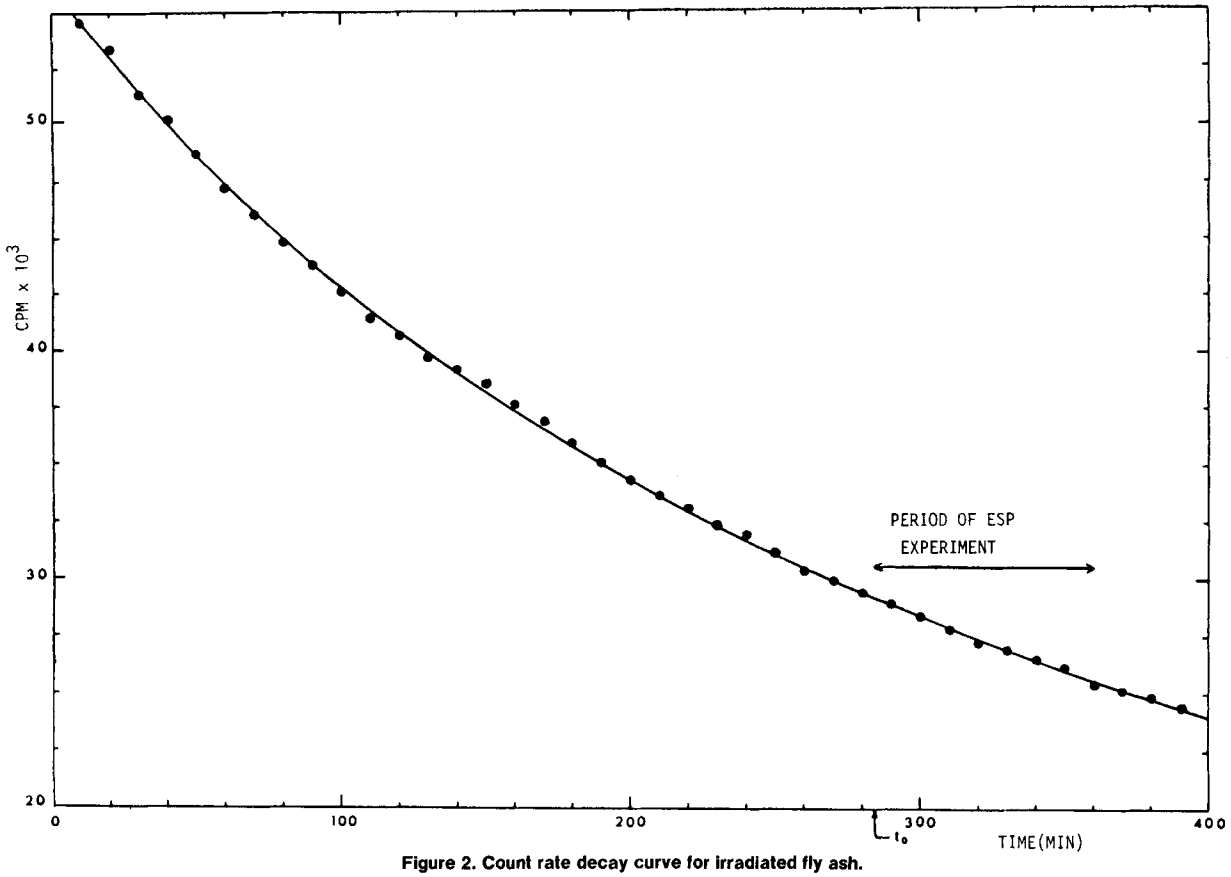

Figure 2. Count rate decay curve for irradiated fly ash.

to the other. A flexible cable passed from the detector out of the ESP to a counting system which consisted of an amplifier (ORTEC 485), timer (ORTEC 719), pulse counter with buffer memory (ORTEC 770), high voltage power supply (ORTEC 456), printout control module (ORTEC 432A), and printer (ORTEC 777A).

In the normal course of its operation the electrostatic precipitator is fed with a suspension of a coal-fired power plant fly ash in air. A sample of this fly ash was irradiated in the 1.0 MW Pulstar nuclear reactor at North Carolina State University for 30 seconds at a flux of 1.5×10^{13} n $cm^{-2} \cdot s^{-1}$, and the irradiated ash was subjected to neutron activation analysis to determine its potential for labeling in tracer experiments. The results of this analysis were reported by Felder and Arce-Medina (1980).

In a second experiment, a 0.5 g fly ash sample was irradiated under the same conditions used for the activation analysis, and the irradiated ash was placed on one side of a 3.175 mm thick stainless steel plate. (The collection plate in the ESP is also 3.175 mm stainless steel.) The scintillation detector was mounted within a lead collimator located roughly 2.5 cm behind the plate (the position to be used in the proposed experiments on the precipitator) and the tracer activity was monitored for 72 hours.

The results of this experiment are shown in Figure 2. The magnitude of the observed activity level indicated that the quantity of fly ash used in this test under the given irradiation conditions would yield a total activity within detection limits for at least eight hours following the time of irradiation. The curve was also used as a basis for correcting measured activities for natural tracer decay.

In experiments performed on the precipitator, a 0.5 g sample of fly ash was irradiated in the nuclear reactor, and the irradiated ash was placed in a 3.7 cm^3 (250 dram) polyethylene vial, with a tightly fitting lid. The vial was placed in a secondary plastic container which was heat-sealed for transportation from the reactor to the electrostatic precipitator. The container was placed in a lead container and remained at the reactor for roughly three hours, during which time the short-lived radionuclides decayed.

The container was then transported from North Carolina State University to the National Environmental Research Center, and was brought to the electrostatic precipitator laboratory. The secondary container was removed under a hood, the heat seal was broken, and the primary vial was removed and inserted bottom first into the receptacle of an injection device, and was locked in. A hollow needle at the base of the receptacle punctured the bottom of the vial. The device was inserted through a side access port in the ESP to a point such that the top of the vial was within the primary gas flow channel of the precipitator, at the same height as the scintillation detector. The total activity of the fly ash never exceeded 100 μCi at the time of transfer to the injector.

To inject the tracer, a quick release valve in an air line to the injector was opened, exposing the vial to a pressure of roughly 650 kPa (80 psig). A burst of compressed air passed through the needle, forced open the vial lid, and blew the labeled fly ash into the precipitator flow channel. The activity subsequently measured at a point on the plate provided a measure of the relative amount of the tracer that had been collected in the vicinity of that point.

In a preliminary experiment carried out before labeled fly ash was injected into the unit, the detector was mounted, the precipitator voltage was turned on, and the detector reading was noted as the voltage was increased in a series of steps. The measured activity remained at background level as long as the voltage was -40 kV or higher, but became totally erratic at more negative applied voltages, indicating electromagnetic interference with the photomultiplier tube on the scintillation detector. All experiments were therefore carried out at -30 kV.

A series of runs was performed to investigate the dependences of the deposition profile and reentrainment rate on air velocity, inlet dust loading, and state of the collection plate (clean or coated with dust). A detailed summary of the conditions in each run is given in Tables 1 (runs with no

TABLE 1. TEST CONDITIONS AND RESULTS FOR THE FRICTION REENTRAINMENT TESTS

Plate Condition	Temp. °C	R.H. (%)	Air Vel. (m/s)	k^* (s^{-1})
Clean	22	83	2.00	0.0693×10^{-3}
Clean	34	61	2.60	0.2318×10^{-3}
Clean	26	89	1.87	0.0847×10^{-3}
Clean	26	89	2.50	0.2045×10^{-3}
Coated	31	57	1.73	0.0132×10^{-3}
Coated	31	57	1.88	0.0167×10^{-3}
Clean	31	77	1.58	0.0218×10^{-3}
Clean	31	77	1.88	0.0575×10^{-3}
Clean	31	77	2.36	0.1267×10^{-3}
Coated	31	77	1.88	0.0372×10^{-3}
Coated	31	77	2.36	0.0633×10^{-3}

* k = reentrainment rate constant

TABLE 2. TEST CONDITIONS AND RESULTS FOR THE IMPACTION REENTRAINMENT TESTS

Plate Condition	Mass Loading Inlet g/m³	Air Vel. m/s	Water Vol. %	Temp. °C	k^* (s^{-1})
Coated	1.776	1.60	2.6	34	0.0588×10^{-3}
Coated	2.196	1.61	2.8	35	0.0863×10^{-3}
Coated	1.923	1.92	2.8	35	0.1670×10^{-3}
Clean	4.289	1.60	2.6	34	0.1638×10^{-3}
Clean	2.703	1.91	2.6	34	0.2382×10^{-3}
Coated	2.950	1.60	2.6	34	0.1572×10^{-3}
Coated	2.907	1.91	2.6	34	0.2903×10^{-3}
Clean	3.238	1.60	3.1	34	0.1238×10^{-3}
Clean	2.520	1.56	2.9	26	0.0637×10^{-3}
Clean	1.870	1.87	2.9	26	0.1327×10^{-3}
Clean	1.680	1.57	3.4	31	0.0163×10^{-3}

* k = reentrainment rate constant

dust loading at the inlet) and 2 (remaining runs). The operating parameters for the precipitator during this series of runs were as follows:

Temperature: 16–35°C (61–95°F)
Relative humidity: 49–89%
Plate spacing: 23 cm (9 in.)
Wire spacing: 23 cm (9 in.)
Applied voltage: −30.5 kV in Stage 2
Stages 1,3,4 off
Gas velocity: 1.6 m/s, 1.9 m/s
Inlet dust loading: 0 g/min, 30 g/min, 60 g/min

The tracer used in all runs was 0.5 g of the same fly ash used as the feed to the precipitator, irradiated for 60 s in the NCSU Pulstar reactor at a power factor of 1 MW and an approximate flux of 1.2×10^{13} n/cm²-s.

Several tests were performed using two detectors, one at the height of the middle port where the injections were made, and the other 30.0 cm above the first one, with the object of determining the extent of radial dispersion of the injected dust. The signal registered by the second detector barely exceeded background, however, indicating that the rate of radial dispersion was too low for a measurable quantity of dust to span the vertical distance between the detectors while traversing a single stage of the precipitator. All results to be reported were therefore obtained with a single detector at the height of the tracer injection port.

Deposition Profiles

The tracer deposition profiles for all runs were obtained by injecting at the inlet of the second stage at a point 3.2 cm from the plate behind which the scintillation detector was mounted, except in Run 22, when the injection was made at the inlet of the first stage. (Illustrative profiles obtained by injecting at different distances from the plate have been shown elsewhere (Felder and Arce-Medina, 1980). The gas flow rate at the moment of injection was turned down to 1.17 m/s from its usual value of 1.60 m/s to minimize the possibility of tracer loss due to friction reentrainment. Following injection, the detector was moved back and forth and the activity was monitored at several horizontal positions by recording the counts in one-minute intervals.

Values of the normalized activity of the deposited tracer are plotted vs. axial position for three of the runs in Figure 3. Profiles for other runs were similar to those shown. It is noteworthy that the deposition profile for Run 22, in which the tracer was injected at the precipitator inlet rather than at the inlet of the second stage, follows the same pattern as do the profiles for the other runs. It is therefore reasonable to assume that the behavior of the dust entering the precipitator is modeled by the behavior of the tracer.

The deposition profile for Run 24, in which the tracer injection was made following the predeposition of dust on the plates, follows the general pattern of the profiles for the other runs, in which the plates were clean prior to injection. A close comparison of all profiles shows, however, that the point of maximum deposition for this run is displaced horizontally to the right, indicating a lowering of the particle migration velocity and a corresponding lowering of the collection efficiency under coated plate conditions.

To apply results of the type given above to the complete analysis of a precipitator or the evaluation of a precipitator model, an extensive series of profiles would be required, with the position of the tracer injection being varied both vertically and horizontally across the flow channel, and the detector position also being varied both vertically and horizontally. The total deposition of dust in the precipitator could then be determined by interpolation and integration of these profiles over the inlet cross section. These experiments were not performed in the present study.

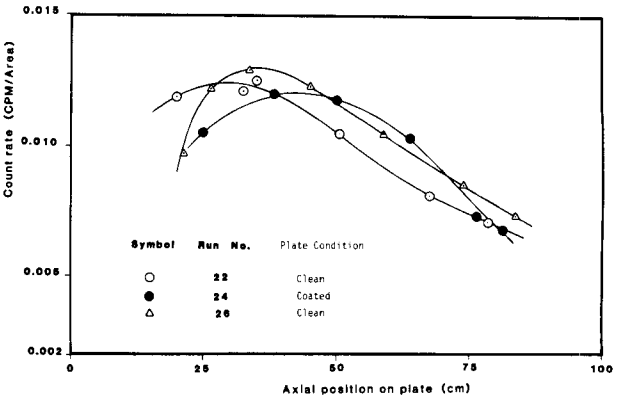

Figure 3. Deposition profiles.

REENTRAINMENT MEASUREMENT

Felder and Arce-Medina (1980) proposed that reentrainment due to gas friction and particle impaction can be modeled as a first-order process:

$$dn/dt = -kn \tag{1}$$

where $n(t)$ is the quantity (mass) of fly ash deposited at a location on the plate within the field of vision of the detector. They showed that if $R(t)$ is the counting rate at some time t, measured from the time of irradiation of the tracer and corrected for background level, and $A(t)$ is the ordinate of the tracer decay curve of Figure 2, then

$$ln\left[\frac{R(t)A(t_o)}{R(t_o)A(t)}\right] = -k(t - t_o) \tag{2}$$

where t_o is an arbitrary time, normally the beginning of the measurement period. A semilogarithmic plot of $(R/R_o)(A_o/A)$ vs. $(t - t_o)$ should thus be a straight line with slope $-k$.

Felder and Arce-Medina (1980) demonstrated the validity of this model, using data from preliminary experiments. They also formulated a statistical test to confirm that the decay in the measured activity level differs (or does not differ) significantly from natural tracer activity decay. The extent of the difference provides a measure of the magnitude of reentrainment. In the test reported, reentrainment by gas friction alone (determined by measuring k under conditions when only clean air flowed past the plate following injection of the tracer) was shown to be negligible at the test condition. Impaction reentrainment was then measured by feeding a dust-laden air past the plate, and calculating k as described above. The value determined was 1.8×10^{-4} s^{-1}.

The significance of this value can be viewed in several ways. Under the conditions of this experiment—namely, an applied voltage of −30 kV, a plate spacing of 23 cm, a gas flow rate of 33 m³/min, and an inlet dust loading of about 1.8 g/m³—it takes roughly 63 minutes for half of the fly ash initially deposited on a clean plate to be reentrained. Put another way, the rate of loss of fly ash at a given instant of time is roughly 1.2%/min.

Friction Reentrainment

Friction reentrainment is caused by shear forces at the interface between the gas boundary layer and the dust layer on the collection plate. It was measured by determining reentrainment rate constants at several gas flow rates with no dust being fed to the precipitator, with the detector mounted at the point of maximum deposition. The measured loss of activity therefore provides a measurement of the net reentrainment rate, defined as the gross reentrainment

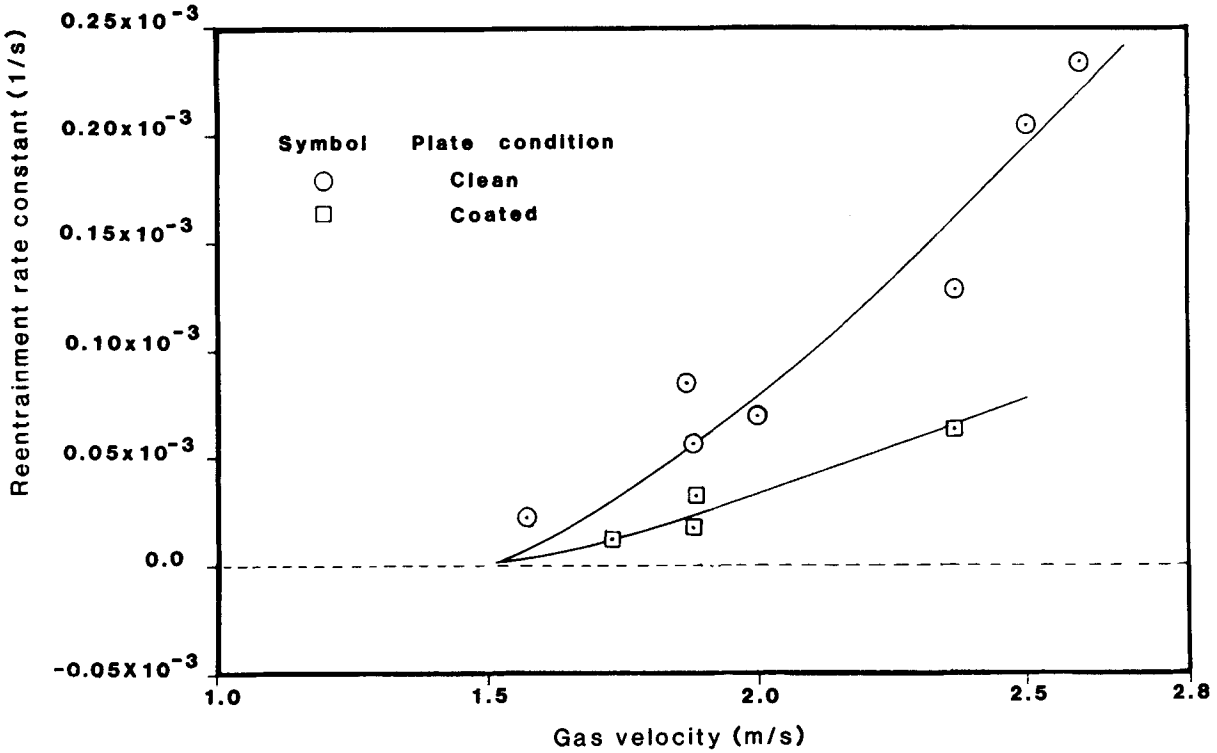

Figure 4. Friction reentrainment rate vs. gas velocity.

rate minus the rate of secondary deposition of previously deposited and reentrained dust.

In the first 21 runs performed, the gas flow rate control system was such that large fluctuations in velocity were commonplace. These fluctuations had the effect of dislodging deposited tracer during the period in which data were being taken, making the results difficult or impossible to interpret. A variable speed fan controller was installed prior to Run 22, and the problem never recurred. Run 22 and subsequent runs were then used to provide the data base for the studies to be described.

The results are summarized in Table 1, and the reentrainment rate constants determined for both clean and coated plate conditions are plotted versus gas velocity in Figure 4. All data points shown in Table 1 are also shown in Figure 4, but those marked with X's were not used in the regression calculations to be described later in this report. The curves shown in the figure were derived from these calculations.

Figure 4 shows that the rate of friction reentrainment increases with increasing gas velocity, as would be expected. An unexpected result is that the rate is lower for a given velocity when a dust layer covers the plate than when the plate is clean. The latter result may be explained in terms set forth by Zimon (1969), who postulated two mechanisms for friction reentrainment: denudation, in which the aerodynamic drag force of the air stream breaks the adhesive bonds between particles and the plate, and erosion, in which the autohesive forces binding an agglomeration of particles are overcome by the drag force. In the present studies, the clean plate reentrainment measurements provide a measure of the rate of denudation, while the coated plate measurements are indicative of the rate of erosion. The results plotted in Figure 4 support the observation of Zimon that autohesive forces are stronger than adhesive forces, so that a greater drag force is needed for the removal of dust particles from coated plates than from clean plates.

Impaction Reentrainment

Experiments similar to those described above were performed with dust being fed to the precipitator following injection of the tracer. The test conditions and results are summarized in Table 2, and plots of the reentrainment rate constant versus dust loading for clean and coated plates are shown in Figures 5 and 6. The points shown on the ordinate axes of these figures (corresponding to zero mass loadings) represent interpolated values of the friction reentrainment rate constant obtained from the data shown in Figure 4. The curves are the products of regression studies to be described.

The rate of impaction reentrainment can be attributed to two characteristics of the system: the momentum carried by the impacting particles, and the collision frequency. For a given particle size distribution, the first of these quantities is proportional to the gas velocity, and the second is a function of the dust loading of the feed gas. Figures 5 and 6 indicate that for both clean and coated plates, increases in both the impact momentum and the impact frequency increase the reentrainment rate.

REENTRAINMENT MODELING

One goal of studies like those described above is the formulation of a predictive model for reentrainment, which can be incorporated into an overall precipitator model. Zimon (1969) has proposed semiempirical formulas for both friction and impaction reentrainment. The paragraphs that follow describe efforts to fit the data shown in Figures 4–6 with Zimon's formulas by logarithmic transformation and linear regression.

Before these calculations are presented, however, we should note that the results cannot be considered general formulas that may be used to predict reentrainment rates for an arbitrary dust in an arbitrary precipitator. To derive such formulas, a great many more experiments would need to be performed, with much better control being exerted over the primary parameters used in this study (gas velocity and inlet dust loading), as well as other potentially important parameters such as temperature and water content of the dust, and the thickness of the dust layer on the plate.

Moreover, even the formulas presented for the specific conditions studied in the present experiments should be regarded as merely exemplary. At least three or four times the number of runs performed would be required to provide statistical significance to the estimated parameters. What the calculations to be presented demonstrate is simply that the given model provides a good basis

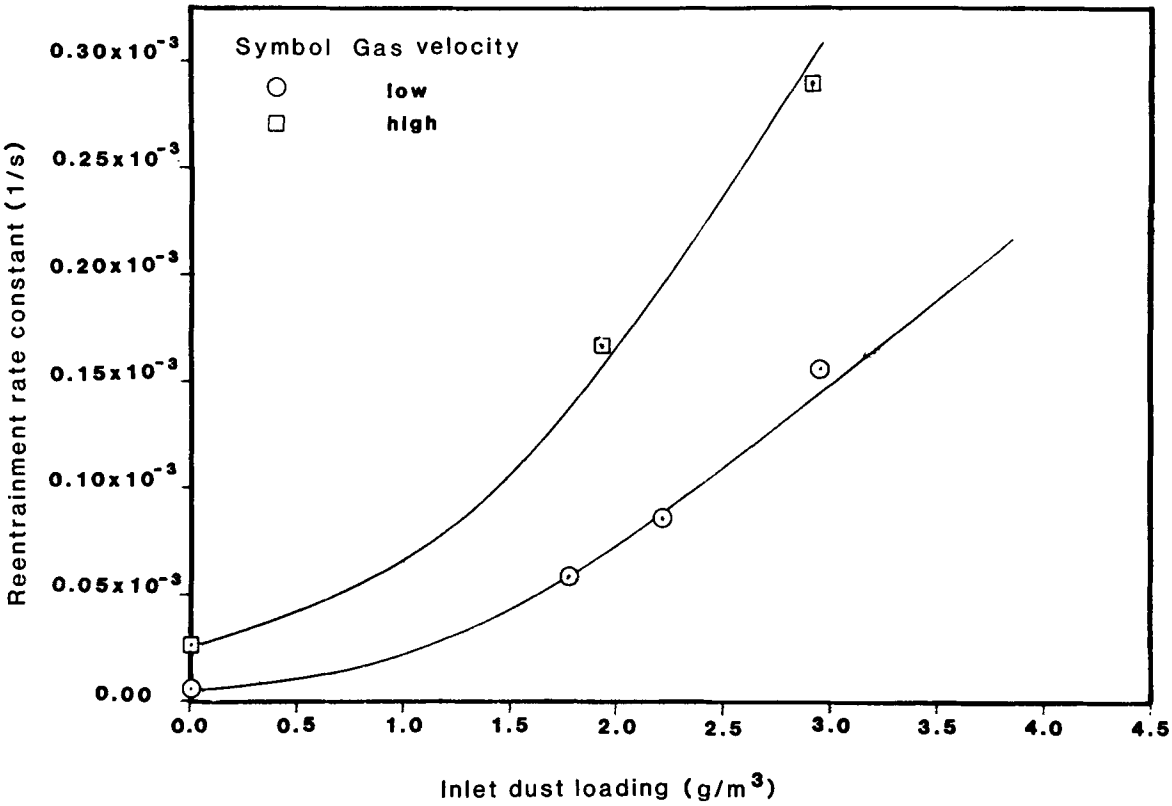

Figure 5. Impaction reentrainment rate vs. dust loading for clean plates.

for correlating reentrainment rates, and that the model parameters have certain orders-of-magnitude. More quantitative conclusions must await the performance of additional experiments.

Zimon (1969) gives the following semiempirical relationship between the friction reentrainment rate and the gas flow velocity:

$$r = b_o(u - u_m)^{\beta 1} \tag{3}$$

where

r = loss rate of dust, g/m²·s
u = average gas velocity, m/s
u_m = minimum velocity for reentrainment, m/s
b_0, β_1 = empirical coefficients

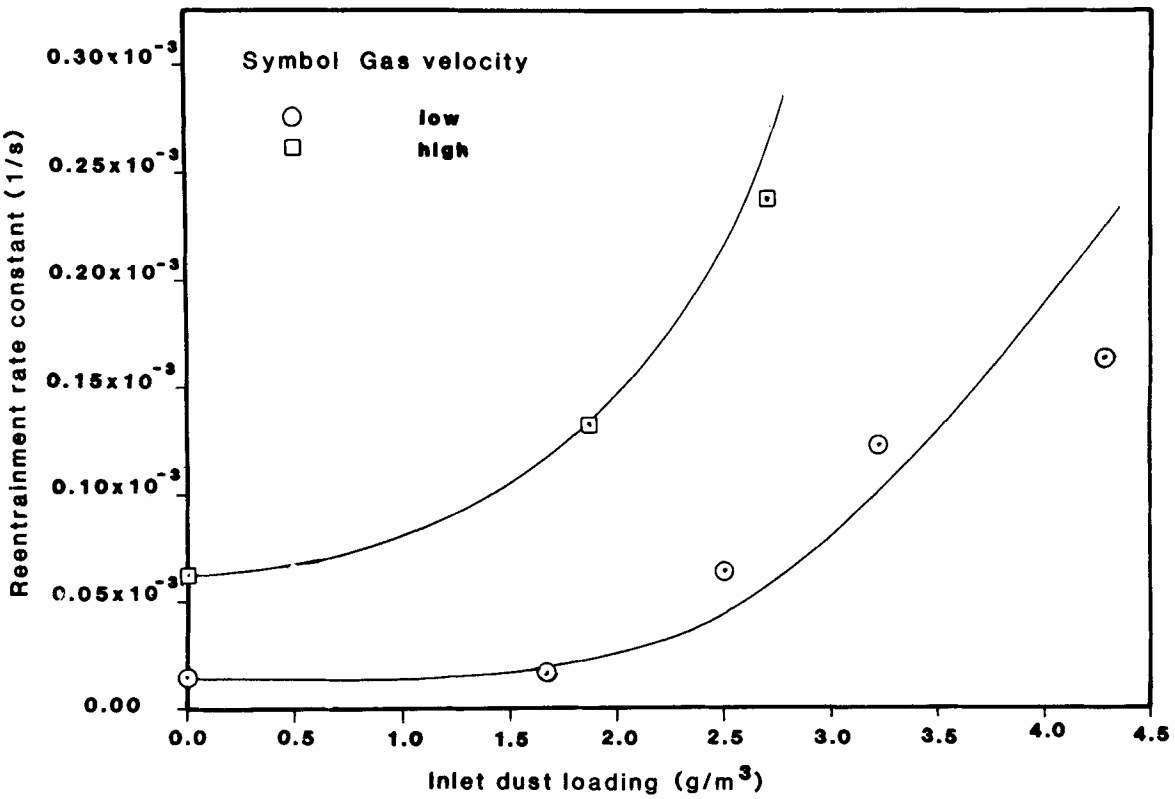

Figure 6. Impaction reentrainment rate vs. dust loading for coated plates.

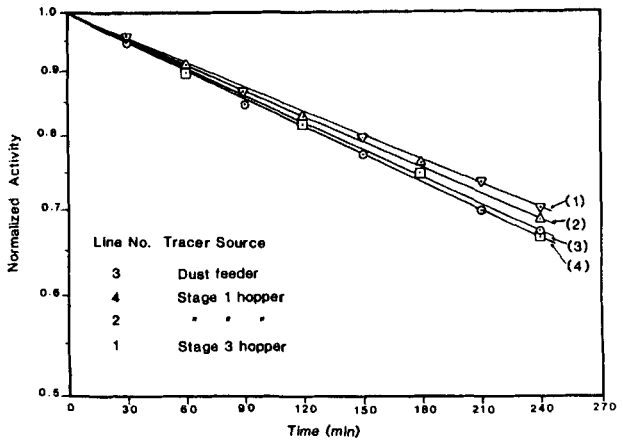

Figure 7. Comparison of tracer activity for fly ashes from different precipitator stages.

The gas flow at which reentrainment starts to occur is seen from Figure 7 to be between 1.25 and 1.7 m/s. Basset et al. (1977) used spherical particles of glass powder with 60–70 μm diameter, and measured a reentrainment threshold of about 1.5 m/s for several voltage-current pairs. Nichols and Gooch (1972) observed somewhat higher values.

To correlate the reentrainment rate data of the present study with Eq. 3, the following transformation is applied:

$$r = -kn_0/\alpha \tag{4}$$

where k, the reentrainment rate constant, has the meaning previously given, n_0 is the quantity of tracer deposited at the arbitrary time t_o, and α is an effective area in which the tracer is deposited. If this expression for r is substituted into Eq. 3, the result is

$$k = b_1(u - u_m)^{\beta 1} \tag{5}$$

where $b_1 = b_0 a/n_0$.

The low-velocity data shown in Figure 4 did not permit the determination of a statistically significant value of u_m, and so the value of this parameter was arbitrarily set at 1.5 m/s. The quantities b_1 and β_1 were treated as adjustable parameters, and were determined by fitting Eq. 5 to the non-crossed-out points on Figure 4, first taking logarithms of the equation and then applying linear regression. The exponent β_1 for both clean and coated plates was close to 1.15. The data were then refitted using this value, with the following results:

$$\text{clean plates: } k = 1.92 \times 10^{-4}(u - 1.5)^{1.15} \tag{6}$$

$$\text{coated plates: } k = 0.76 \times 10^{-4}(u - 1.5)^{1.15} \tag{7}$$

where k is in s^{-1} and u is in m/s. The solid curves in Figure 4 are plots of Eqs. (6) and (7).

The agreement between prediction and measurement shown in Figure 4 is fairly good. While as noted previously the particular values of the coefficients of Eqs. 6 and 7 cannot be applied to a wide variety of conditions in the absence of a great deal more experimentation, it seems reasonable to make the following inferences:

1. The relationship of Eq. 5 provides a good basis for correlating the friction reentrainment rate constant with gas velocity.
2. The minimum velocity required for friction reentrainment under the conditions of the present study is roughly 1.5 m/s.
3. For both clean and coated plates, the reentrainment rate constant varies approximately as the 1.15 power of the difference between the actual gas velocity and the minimum velocity required for reentrainment.

The next step in the analysis is to correlate measured rates of impaction reentrainment. Zimon (1969) proposed a modified version of the expression of Eq. 5 to account for both friction and impaction reentrainment. In terms of the reentrainment rate constant, this expression may be written in the form

$$k = b_1(u - u_{m1})^{\beta 1} + b_2(u - u_{m2})C^{\beta_2} \tag{8}$$

where C is the dust content of the air in g/m^3. (Zimon's formula specified $\beta_2 = 1$; data to be shown clearly indicate a nonlinear dependence on dust loading.)

The data shown in Figures 5 and 6 were fitted with Eq. 8. For both clean and coated plates, the parameters b_1, u_{m1}, and β_1 were fixed at the values determined from the friction reentrainment measurements. The minimum velocity for impaction reentrainment, u_{m2}, is likely to differ from that for friction reentrainment u_{m1}. For both clean and coated plates, several values of u_{m2} were tried. For each value, the parameters b_2 and β_2 were determined by subtracting the term for friction reentrainment from both sides of Eq. 8, taking logs of both sides, and applying linear regression to the data shown in Figures 5 and 6. The results were as follows:

$$\text{clean plates: } k = 1.92 \times 10^{-4}(u - 1.5)^{1.15} + 0.28 \times 10^{-4}(u - 1.5)C^3 \tag{9}$$

$$\text{coated plates: } k = 0.76 \times 10^{-4}(u - 1.5)^{1.15} + 0.62 \times 10^{-4}(u - 1.3)C^2 \tag{10}$$

The solid curves on Figures 5 and 6 are plots of Eqs. 9 and 10. The agreement between prediction and measurement is seen to be fairly good, but this is not surprising in view of the relatively small number of data points available for model parameter estimation.

A final point is worth noting concerning the observed scatter in the measured values of reentrainment constants. The resistivity of the dust layer is bound to have an effect on the forces binding the particles to the plate. The resistivity in turn is strongly dependent on the temperature and water content of the gas flowing through the precipitator, and may span several orders of magnitude at ambient temperatures as the water content of the dust varies from 0 to about 20%. This information cannot be used quantitatively to interpret our data; however, it seems likely that the variations in the temperature and humidity noted in Tables 2 and 3 would be responsible in part for the observed data scatter.

Having pointed out the danger in deriving overly broad inferences from the modeling results presented above, based as they are on such limited data, we would venture to draw the following tentative conclusions:

1. The model proposed by Zimon which adds the contributions of friction and impaction reentrainment to determine the total reentrainment provides a reasonable basis for data correlation. However, the impaction reentrainment rate varies nonlinearly with the dust concentration (approximately as the square of the concentration for coated plates and the cube for clean plates).
2. The minimum velocity required for impaction reentrainment from clean plates is roughly the same as that for friction reentrainment (1.5 m/s). The minimum velocity for coated plates is lower than that for clean plates.

TABLE 3. TRACE ELEMENT CONCENTRATION AT DIFFERENT ESP LOCATIONS (mg ELEMENT/g SAMPLE)

Element	Dust Feeder	Stage 1 Hopper	Stage 3 Hopper
As	0.013	0.008	0.008
Br	0.028	0.005	0.004
Na	4.499	4.340	3.747
K	9.233	6.624	6.176
Ce	0.090	0.109	0.129
Th	0.020	0.026	0.030
Cr	0.056	0.055	0.053
Ba	3.287	3.714	4.670
Cs	0.004	0.005	0.006
Sc	0.017	0.017	0.020
Fe	23.1784	24.540	29.191
Co	0.015	0.014	0.015

TABLE 4. SLOPES OF TRACER DECAY CURVES FOR DIFFERENT DUSTS

Sample Location	$m \times 10^3$	$s \times 10^5$	r
Dust Feeder	−1.67	2.38	0.990
Stage 1 Hopper	−1.48	1.82	0.993
Stage 1 Hopper	−1.68	1.84	0.994
Stage 3 Hopper	−1.56	1.90	0.956

m = slope
s = standard deviation
r = correlation coefficient

PARTICLE SIZE EFFECTS ON ACTIVITY DECAY RATES

In the tracer studies, the measured loss of activity must be corrected for the rate of natural activity decay, using the curve shown in Figure 2. The presumption associated with this procedure is that there is a unique decay rate for the fly ash used as the tracer; in particular, the ash fed to the precipitator (a sample of which was used to generate the data of Figure 2) decays at the same rate as the ash collected on the plate.

Several investigators (Davison et al., 1974; Ondov et al., 1979) have shown that the concentration of trace elements in coal fly ash particles is a function of particle size. Since the particle size distribution of collected and uncollected fly ash will inevitably shift toward smaller particles in the direction of flow along the precipitator, the isotopic composition and hence decay rate might also be expected to vary, leading to errors in tracer measurement data interpretation.

Fly ash samples from the dust feeder, the first stage collection hopper, and the third stage collection hopper were irradiated, and their activity was monitored through a 3.175 mm stainless steel plate. Semilog plots of the data are shown in Figure 7 for a period of time between 6 and 10 hours after irradiation. Each of these plots was subjected to linear regression, with the results shown in Table 4.

These results indicate that there is relatively little difference between the normalized decay curves of the dust collected near the inlet and near the outlet of the precipitator, and that it is consequently appropriate to use the decay curve of Figure 2 for all corrections. This was confirmed by recalculating a number of measured reentrainment rates using the other curves of Figure 7, and showing that the calculated values were essentially independent of which decay curve was used.

It might be inferred from these results that the concentrations of the isotopes which affect the decay curve for $6\text{ h} < t < 10\text{ h}$ must be more or less the same in all three dusts, despite the probable differences in the particle size distribution of the dusts. To confirm this inference, samples of the dusts were subjected to neutron activation analysis, and concentrations of the elements principally responsible for the measured activity in the tracer experiments were determined. The results are shown in Table 3. They indicate that within the range of experimental precision, the isotopic compositions of dusts collected at every stage of the precipitator are indeed comparable.

ACKNOWLEDGMENTS

This research was supported by U.S. Environmental Protection Agency Grant No. R805404011. The research has not been subjected to the Agency's required peer and policy review and therefore does not necessarily reflect the views of the Agency, nor does mention of trade names or commercial products constitute endorsement or recommendation for use.

The authors express their thanks to Kuruvilla Verghese for assistance in planning and implementing the experiments; to the N.C. State nuclear reactor staff for the tracer preparation and the loan of area monitoring instruments; to Thomas Gerig for assistance with statistical analysis; and to Geddes Ramsey for assistance with the precipitator operation. Thanks are also extended to the National Council of Science and Technology of Mexico (CONACYT) for fellowship support of E. Arce-Medina.

NOTATION

$A(t)$ = measured counting rate for irradiated fly ash, cpm
a = effective area in which the tracer is deposited, m^2
b_o = empirical coefficient in the friction reentrainment model, g/m^2
b_1 = empirical coefficient in the friction reentrainment model, dimensionless
C = dust content of air, g/m^3
k = reentrainment rate constant, s^{-1}
$n(t)$ = mass of fly ash deposited on the plate within the field of vision of the detector, g
$R(t)$ = count rate of deposited tracer, cpm
r = loss rate of dust, $g/m^2 \cdot s$
t = time, s
u = gas velocity, m/s
u_m = minimum velocity for reentrainment, m/s (u_{m1} for friction, u_{m2} for impaction)

Greek Letters

β_1 = empirical coefficient in the equation for friction reentrainment, dimensionless
β_2 = empirical coefficient in the equation for impaction reentrainment, dimensionless

LITERATURE CITED

Arce-Medina, E., "The Modeling of a Pilot-Scale Electrostatic Precipitator," Ph.D. Thesis, North Carolina State Univ., Raleigh (1982).

Basset, J. D., K. Akutzu, and S. Masuda, "A Preliminary Study of Reentrainment in an Electrostatic Precipitator," *J. Electrostatics*, **3**, 311 (1977).

Davison, R. L., D. F. S. Natusch, J. R. Wallace, and C. A. Evans, Jr., "Trace Elements in Fly Ash: Dependence of Concentration on Particle Size," *Environ. Sci. Technol.*, **8**, 1107 (1974).

Felder, R. M., and E. Arce-Medina, "Radiotracer Measurement of Particle Deposition and Reentrainment in an Electrostatic Precipitator," *Intl. J. Appl. Rad. Isotopes*, **31**, 761 (1980).

Lawless, P. A., B. E. Daniel, and G. H. Ramsey, "Characterization of the EPA/IERL RTP Pilot-Scale Precipitator," U.S. EPA Report, 600/7-79-052 (1979).

Nichols, G. B., and J. P. Gooch, "An Electrostatic Precipitator Performance Model," U.S. EPA Report, 650/2-74-132 (1974).

Oglesby, Jr., S., and G. B. Nichols, *Electrostatic Precipitation*, Marcel Dekker, New York (1978).

Ondov, J. M., R. C. Ragaini, and A. H. Biermann, "Emissions and Particle Size Distribution of Minor and Trace Elements at Two Western Coal-Fired Power Plants Equipped with Cold-Side Electrostatic Precipitators," *Environ. Sci. Technol.*, **13**, 946 (1979).

Zimon, A. D., *Adhesion of Dust and Powder*, Plenum Press, New York (1969).

Manuscript received March 9, 1983; revision received September 15, and accepted September 26, 1983.